



Mechanical Unfolding of Alpha- and Beta-helical Protein Motifs

Journal:	<i>Soft Matter</i>
Manuscript ID	SM-ART-10-2018-002046.R1
Article Type:	Paper
Date Submitted by the Author:	28-Nov-2018
Complete List of Authors:	DeBenedictis, Elizabeth; Northwestern University Keten, Sinan; Northwestern University, Mechanical Engineering

SCHOLARONE™
Manuscripts



Mechanical Unfolding of Alpha- and Beta-helical Protein Motifs

E. P. DeBenedictis and S. Keten*

Received 24th September 2018,
Accepted 00th January 20xx

DOI: 10.1039/x0xx00000x

www.rsc.org/

Alpha helices and beta sheets are the two most common secondary structure motifs in proteins. Beta-helical structures merge features of the two motifs, containing two or three beta-sheet faces connected by loops or turns in a single protein. Beta-helical structures form the basis of proteins with diverse mechanical functions such as bacterial adhesins, phage cell-puncture devices, antifreeze proteins, and extracellular matrices. Alpha helices are commonly found in cellular and extracellular matrix components, whereas beta-helices such as curli fibrils are more common as bacterial and biofilm matrix components. It is currently not known whether it may be advantageous to use one helical motif over the other for different structural and mechanical functions. To better understand the mechanical implications of using different helix motifs in networks, here we use Steered Molecular Dynamics (SMD) simulations to mechanically unfold multiple alpha- and beta-helical proteins at constant velocity at the single molecule scale. We focus on the energy dissipated during unfolding as a means of comparison between proteins and work normalized by protein characteristics (initial and final length, # H-bonds, # residues, etc.). We find that although alpha helices such as keratin and beta-helices CsgA and CsgB can require similar amounts of work to unfold, the normalized work per hydrogen bond, initial end to end length, and number of residues is greater for beta-helices at the same pulling rate. To explain this, we analyze the orientation of the backbone alpha carbons and backbone hydrogen bonds during unfolding. We find that the larger width and shorter height of beta-helices results in smaller angles between the protein backbone and the pulling direction during unfolding. As subsequent strands are separated from the beta-helix core, the angle between the backbone and the pulling direction diminishes. This marks a transition where beta-sheet hydrogen bonds become loaded predominantly in a collective shearing mode, which requires a larger rupture force. This finding underlines the importance of geometry in optimizing resistance to mechanical unfolding in proteins. The helix radius is identified here as an important parameter that governs how much sacrificial energy dissipation capacity can be stored in protein networks, where beta-helices offer unique properties.

Introduction

As essential building blocks in biological systems, proteins can be found in a vast array of sizes and shapes and serve a diverse range of functions. While some proteins are needed for signaling or enzymatic purposes, many different proteins play a structural role and serve load-bearing functions within cells and in the extracellular matrix (ECM). The function and mechanical properties of many proteins are dictated by their folded shape, determined by primary sequence. Protein-based structures are hierarchical, composed of distinct structures at multiple length scales (such as secondary, tertiary, quaternary structures and beyond). This feature allows for tailored mechanical responses that are more complex than nonhierarchical materials and can often be difficult to replicate synthetically. For example, soft biological materials made up of helical proteins exhibit non-linear force extension curves and can tolerate flaws during fracture by allowing geometric transformation of a crack tip, reducing stress concentrations¹. The influence of architecture on mechanics can be seen on scales ranging from the large to the minute. For example, on the macroscale, F-actin networks composed of the same constituent fiber but with differences in degree of crosslinking will display different mechanical properties². The power of architecture extends to even smaller

scales, such as within the alpha and beta protein motifs. For isolated protein segments of similar sizes, the tensile response of alpha-helices and beta-sheets differ³, and also depend on the direction of the applied force⁴. As a way to better connect structure and function and to enable use of proteins for bioengineering applications, the mechanical behavior of various secondary and tertiary structures has been the subject of great focus.

Alpha helices and coiled coils are particularly well-studied from a mechanical standpoint as they form the basic constituent of myriad load-bearing networks in cells and ECM. In structural applications, single helices often arrange into groups forming fibrils, and these fibrils arrange themselves to form networks. When under tension, alpha helices exhibit typical three-regime force-extension curves that begin with (1) extension at small forces due to molecular rearrangement without any bond breakage, (2) elongation with linearly increasing work as hydrogen bonds are sequentially broken, and (3) end with dramatic strain stiffening when all original hydrogen bonds have broken and the backbone is covalently stretched⁵. The ability to maintain stability and resist or recover from large deformations is needed for alpha-helical containing proteins such as alpha-keratin⁶, coiled coils in myosin⁷, spectrin⁸, vimentin⁹, and more. The mechanics and stability of alpha helix proteins are of particular interest for applications such as drug delivery via micelles, protein therapy, or use as polymers in hydrogels.

Another main protein motif, beta-strands, are formed between adjacent elongated peptides which form hydrogen bonds across

*Department of Civil and Environmental Engineering and Mechanical Engineering, Northwestern University, Evanston, Illinois 60208, USA. Email: s-
keten@northwestern.edu*

Electronic Supplementary Information (ESI) available: [details of any supplementary information available should be included here]. See DOI: 10.1039/x0xx00000x

their backbones. Beta sheets can be found in structures like silk or amyloid fibrils to provide structural rigidity. The hydrogen bond network among strands has proven useful when hydrogen bonds are broken concurrently¹⁰, and is particularly strong in lateral shear when load is applied in a direction orthogonal to the hydrogen bond, that is, along a beta-strand³.

A hybrid between beta-sheets and helical motifs is the beta helix (or solenoid). Here, adjacent beta strands form a sheet, yet are part of one continuous protein sequence connected by loops or turns. These motifs are found in antifreeze proteins¹¹, viral adhesins¹², tailspike proteins of bacteriophages¹³, and functional amyloids called curli¹⁴, which form the backbone of biofilm extracellular matrices (ECM) formed by certain bacteria including *E. coli*. In some applications the purpose behind certain architectural features is clear: antifreeze proteins are able to provide a nucleation site for water molecules such that ice formation is prevented¹¹, and bacteriophages possess a hollow triangular core allowing compression and puncture of cell membranes¹⁵. For the functional amyloid curli, a comprehensive explanation as to how the structural features of curli are especially suited to serving the function of a the biofilm ECM remains elusive. Nevertheless, curli fibers are known to have high mechanical rigidity and as such have been engineered for applications such as underwater adhesives^{16, 17}, coatings on polymeric surfaces for controlled MOF growth¹⁸, and reinforcement in alginate hydrogels¹⁹.

Quantifying the mechanical response of various protein structures is now possible using both experimental and computational techniques. In experiment, atomic force microscopy (AFM) is commonly used to extend proteins and record the force response from the AFM tip^{7, 20-22}. For example, beta-helical (or beta-solenoid) proteins have been probed using this technique and have found typical sawtooth patterns, where unfolding each repeat occurs in a stepwise fashion beginning at protein extremities²². When a single protein is unfolded multiple times, multiple pathways can be observed that are traversed with varying probabilities, indicating proteins do not necessarily have a single unfolding path²⁰. Beta-rich structures are stabilized by a network of hydrogen bonds, and other structural features such as stacked aromatic residues can also form barriers that resist unfolding^{20, 23}. High forces are necessary to fully unfold these motifs and increasing speeds result in increasing ultimate tensile strengths^{24, 25}. AFM studies have also found that proteins rich in beta-structures require higher forces to deform than purely alpha helical proteins. However, these investigations typically involve larger molecules which incorporate impacts of tertiary stabilization between multiple components in addition to individual motifs. Additionally, the tensile response of a single beta-helix has not yet been directly compared with alpha-helices, although many beta-sheet rich motifs have been studied²⁶⁻²⁸.

Computational analysis of protein mechanics can allow the study of molecular detail not easily available through experiment. This can include examination of changes in conformation, force, and energy throughout extension, which are possible to obtain using methods like Steered Molecular Dynamics (SMD) and Umbrella Sampling (US). Although the extension rates in computational work are typically faster than in experiment, many mechanical properties can be calculated in

agreement with experiment²⁹ and unfolding simulations have found the same rate-dependence as seen in experimental studies. Computational techniques have also been used to obtain moduli and persistence lengths for protein structures³⁰. Using simulation, several factors have been found to influence mechanical response, including molecular packing³⁰, hydrogen bond density²⁸ and stress concentration³¹, alignment with force⁴, and secondary structure³. In investigations of secondary structure, individual motifs have typically been used, and have found unfolding alpha helices requires more force than separating bundled helices, and that beta-sheets better resist applied force in shearing than peeling³. In fracture, groups of 3-4 hydrogen bonds have been found to be optimal for mechanical stability (based on parameter insensitivity)³². When under lateral load (bending), beta-helices possess persistence lengths orders of magnitude higher than alpha helices²⁷. Still, the performance of beta-helical structures in comparison to alpha helical structures under tensile load is not fully understood.

As two main structural motifs in proteins, alpha- and beta-motifs differ not just in mechanical response but several other parameters as well, such as like common primary sequence patterns, solubility, and ability to maintain stability in harsh environments, which can dictate or limit the range of function possible. Despite these differences, alpha and beta motifs can be found together in larger structures, and purely alpha-helical or purely beta-sheet motifs can be found in similar roles. For example, both alpha- and beta-helices can form filaments that appear in networks, where they are subjected to both bending and stretching. This raises the question of why one secondary structural motif may be chosen over the other for certain biological functions. As other factors (like sequence, chemistry, solubility) can guide this choice, we ask: what are the mechanical implications of choosing one helical motif over the other? How may either helix be better suited to specific loading scenarios?

Here we aim to explain the differences in mechanical response between various helical protein structures and the properties underlying these differences. Alpha helices (including keratin, a single peptide from a coiled coil, and single vimentin helices) and beta helices (including CsgA and CsgB from the biofilm extracellular matrix fiber curli) are subjected to tensile deformation at a constant velocity until all backbone hydrogen bonds are broken. We compare each protein on the basis of total work to completely unfold and normalize this work by properties of each individual protein, including number of residues and maximum strain. The role of reorientation during unfolding is also studied to explain differences in normalized work. These results shed light on mechanical differences in energy dissipation between alpha- and beta-helices originating from differences in geometry.

Methods

Protein Models

The protein structures used in this study obtained through the Protein Data Bank were keratin (PDB ID: 3tnu), vimentin (PDB ID: 3klf), and a single helix of the coiled coil (PDB ID: 1coi). Beta-helical structures CsgA and CsgB were both obtained from a previous work³³. A table summarizing properties of each protein can be found in Table 1. Each protein was initially oriented such that the helix axis was aligned with the Y axis. Proteins were solvated and ionized to reach a neutral charge. Simulation box sizes were calculated from the maximum extended length of the protein plus an additional 12 Angstroms of padding in each direction.

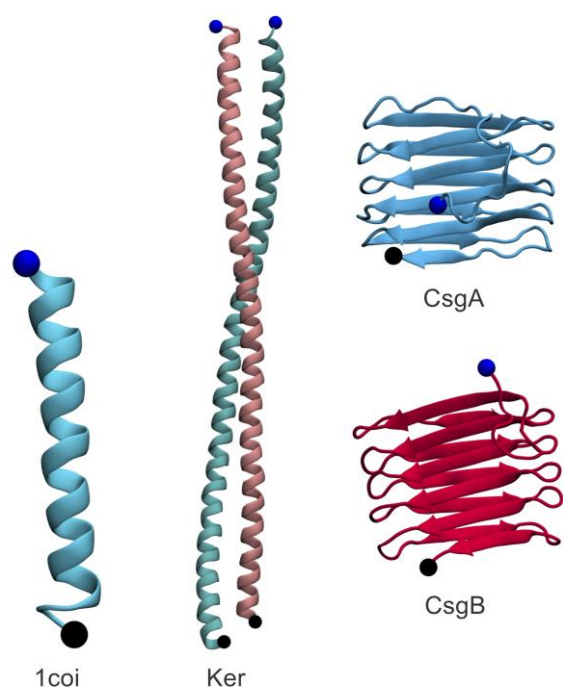


Figure 1. Proteins before force is applied. C-terminal alpha carbons are marked with a black sphere and are held fixed throughout the simulation; N-terminal alpha carbons are marked with a blue sphere and are pulled upward at constant velocity. Proteins are aligned such that their helix axis is along the 010 direction; force is also applied along the 010 vector.

Simulation Setup and Protocol

Constraints were applied by fixing the C-terminal alpha carbon

	Initial Length (Å)	Extended Length (Å)	Maximum Strain	# N-O Backbone H-Bonds	# Residues
CsgA	24.3	497.8	19.5	38	131
CsgB	24.1	494.0	19.5	51	130
Alpha-helix (1coi)	39.3	110.2	1.8	16	29
Keratin	135.5	361.0	1.7	131	185

Table 1. Initial properties of each protein tested, including initial and extended length, maximum strain, backbone hydrogen bonds, and number of residues. See Methods for a description of how these properties are calculated.

and pulling the N-terminal alpha carbon with a spring. For keratin, residues 421 (segment P1) and 476 (segment P2) were

held fixed, and residues 332 (segment P1) and 382 (segment P2) were pulled. For the 1coi helix, residue 29 was held fixed and residue 1 was pulled. For CsgA and CsgB, residues 131 and 130 were held fixed, respectively, and residue 1 was pulled for both. In visualizations of the proteins, the N-terminal alpha carbon is depicted as a blue sphere, and the C-terminal alpha carbon as a black sphere.

SMD Protocol and End of Unfolding

Explicit solvent simulations were run in NAMD³⁴, with periodic boundary conditions under the NPT ensemble at a constant pressure of 1 atm and temperature of 300K. Simulations were run at 1 fs/time step. The latest CHARMM 36 parameter set is used^{35, 36}, with the smooth particle mesh Ewald technique for electrostatics calculations³⁷ and the standard Lennard-Jones potential for nonbonded interactions as implemented in NAMD.

To prepare the protein structures for production simulation, multiple rounds of energy minimization and equilibration were conducted. First, all alpha carbon atoms of the protein were fixed, and 10,000 steps of energy minimization and 100,000 steps of equilibration were conducted. Next, the alpha carbons of the protein were constrained lightly with a 0.05 spring constant (kcal/mol/Å²) and 1 ns of equilibration was conducted. Next, the C-terminal alpha carbon of each peptide was held fixed and the rest of the protein was free during 10,000 steps of energy minimization and 1 ns of equilibration. Finally, during the SMD protocol, the N-terminal alpha carbon of each peptide was pulled with a spring constant of 50 kcal/mol/Å². Pulling speeds tested range from 0.1 m/s to 5 m/s. For each simulation, data was recorded at 10 ps intervals. Proteins are considered unfolded when no backbone hydrogen bonds exist for 50 continuous ps.

Analysis

Force output and work to unfold were analyzed for each trajectory. Work was integrated from force-displacement curves using the trapezoidal method. For every protein, the potential of mean force (PMF) is calculated using SMD output³⁸ according to:

$$F_{\lambda(\tau)} - F_{\lambda(0)} = \langle W(\tau) \rangle - \frac{\beta}{2} (\langle W(\tau)^2 \rangle - \langle W(\tau) \rangle^2) \quad (1)$$

$$\beta = \frac{1}{k_B T} \quad (2)$$

Simulations were visualized using VMD and analyzed using tcl scripts in VMD³⁹. Hydrogen bond calculations were calculated for nitrogen and oxygen backbone atoms only using a 4 Å distance cutoff and 30 degree angle cutoff. The number of backbone hydrogen bonds in each initial protein structure was calculated by averaging the number occupied hydrogen bonds during the last 1 ns round of equilibration, when only the C-terminal alpha carbon is fixed. The angle of each hydrogen bond was based off of the vector connecting the xyz coordinates of the hydrogen atom and the acceptor atom and the O1O vector. Backbone angles were measured using the vector connecting the alpha carbons of the adjacent residue alpha carbons, and were thus not calculated for terminal residues. Initial length was measured as the distance from the C-terminal alpha carbon to the alpha carbon in the first residue in the first repeat in the amyloid core for beta-helices, as the N-terminal 22 residues are unstructured for CsgA and CsgB. For keratin and 1coi, the initial length is measured as the distance from each C-terminal alpha carbon to the N-terminal alpha carbon. Keratin contains two alpha helices, and the initial lengths (132.7 Å and 138.3 Å) are averaged to obtain the value in the table. Keratin has a total of 185 residues as it is comprised of two protein segments with 90 and 95 residues each. Extended length is computed by multiplying the number of residues by 3.8 Å. This is not necessarily the length at which the simulation is terminated, as this depends on the breaking of backbone hydrogen bonds. Strain is calculated as the change in length (from initial to extended length) over the initial length.

Results

To investigate mechanical response of alpha and beta helices under applied force, we conduct pulling experiments at constant velocity. A visualization of each protein before helix extension can be found in Fig 1 and snapshots during extension can be found in Fig S1 and S2 for alpha and beta helices, respectively. First, we compare the total work to unfold as measured by integrating force-displacement curves for each trial and obtaining the potential of mean force (PMF, see Methods). Here, we seek to define what differences exist in energy dissipation during the unfolding of alpha and beta-helices, the physical origins of these differences, and how they may be suited to particular functions.

Potential of Mean Force

The potential of mean force (PMF) shows the change in free energy surface along a particular reaction coordinate. The PMF is plotted as a function of displacement of the pulled terminus and can be found in Fig 2 for each protein tested. First, it is apparent that both beta-helices CsgA and CsgB can reach larger strains while having much shorter initial lengths than the keratin helices tested. The CsgA and CsgB beta helices contain beta-strands of 8 residues connected by turn regions with 3-4 residues, resulting in 22-24 amino acids and substantial “hidden length” per turn. Alpha helices, alternatively, contain only 4 residues per turn. By comparing initial to fully extended lengths, alpha helices can only reach strains of ~1.8, while the beta-helices tested can reach strains of ~19.5. For applications where the protein may fully unfold, the difference in maximum strain

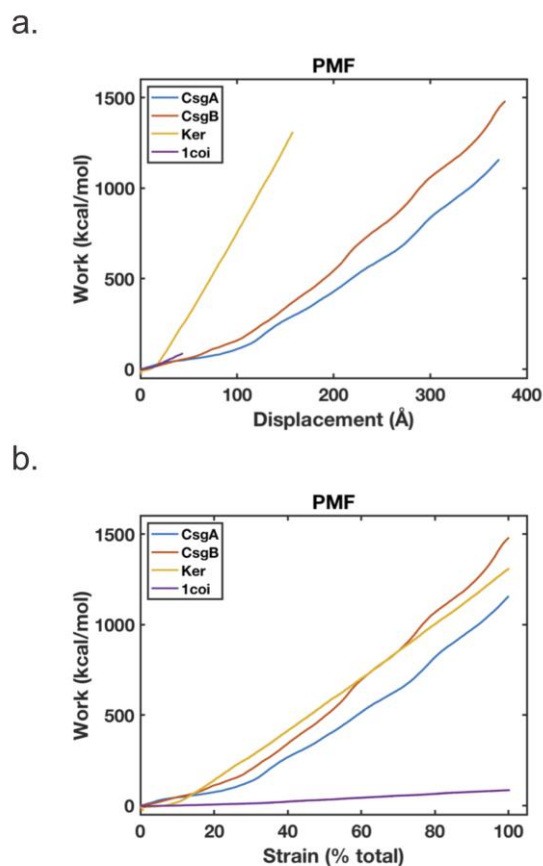


Figure 2. Potential of mean force for each protein during unfolding against displacement (a), and normalized strain fraction (b). First, it is apparent that both beta-helices CsgA and CsgB can reach larger displacements despite having a shorter initial length than the keratin helices tested (keratin contains two parallel helices).

alone may guide the use of a particular type of helix to suit either a low or high strain regime. Alpha-helical components could be used as a type of fine resolution ‘strain gauge’, whereas beta-helical components may be suited to dissipating as much energy as possible, where larger deformations are acceptable or necessary. The keratin PMF shape has a characteristic “toe-heel” shape during unfolding, which first involves molecular rearrangement without breaking backbone hydrogen bonds. This initial region has a brief increase in strain at low work, followed by a linear increase in work with increasing strain. CsgA and CsgB, however, have “waves” within their PMFs, corresponding to unfolding of subsequent repeat loops.

Total Work to Unfold

The total work to fully break all backbone hydrogen bonds is obtained for each trial. These values can be found in the first column of Table 2, and in Fig 3a. From this analysis, CsgB requires the most work to unfold, followed by keratin, and CsgA. The 1coi peptide requires much less work to unfold, as it has the fewest residues. The work to unfold single alpha helices of varying sizes (including each keratin helix alone, and four helices of vimentin) was also calculated. For single helices, a length dependence is noted where increasingly long helices require more work to unfold per residue (Fig S3 and S4). The size-dependence of work to unfold underlines that differences in

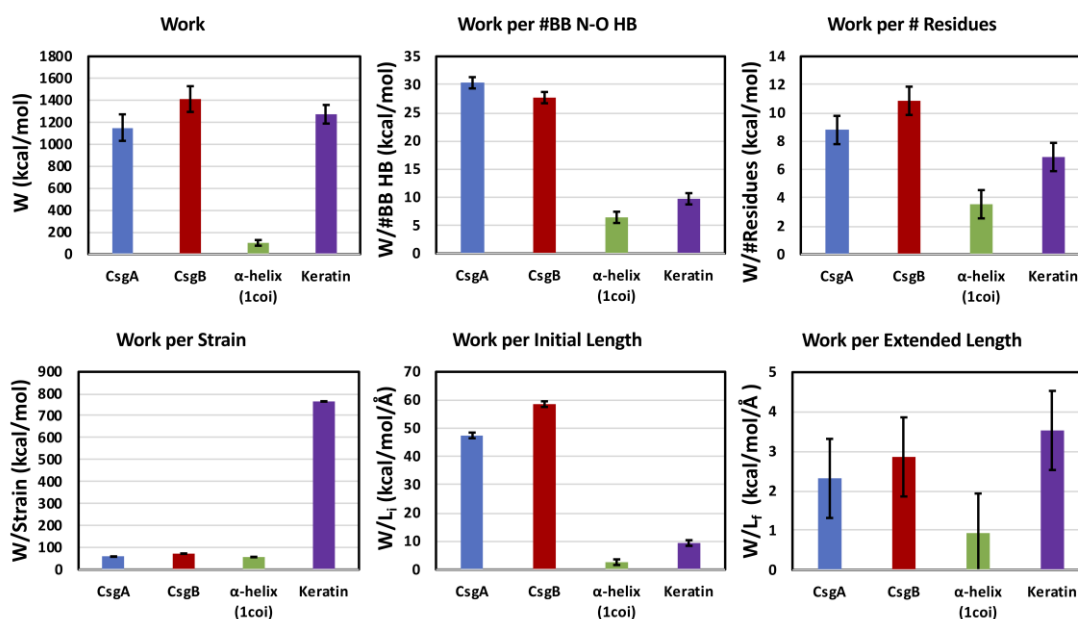


Figure 3. Work and normalized work to unfold for each protein tested. Error bars denote standard deviation between trials.

initial protein properties must be considered to compare each system. Additionally, velocities ranging from 1 – 5 nm/ns were also tested for CsgA and keratin only. A velocity-dependent work to unfold was observed, in agreement with previous studies^{8, 15, 24} (see SI, Fig S6). For velocities 1 m/s and 2.5 m/s, keratin required a higher total work to unfold than CsgA, although at 5 m/s, CsgA required a higher total work to unfold. For the same velocity, CsgA is extended at a higher strain rate due to initial geometry, where the ratio of extended length to initial length is much higher for CsgA (~20.5) than for Keratin (~2.7, see SI for more details).

Normalized Work to Unfold

The work to unfold is studied in the context of protein properties such as initial and final lengths, number of residues, and number of backbone hydrogen bonds in the initial state. As previously noted, beta-helices contain more residues in each repeat, leading to larger hidden lengths and maximum strains when fully unfolding the protein. While the 1coi peptide is tested while removed from its coiled coil, keratin consists of two wrapped alpha helices that are pulled concurrently. Keratin experiences an alpha to beta transition when stretched, as backbone hydrogen bonds within each segment are broken and subsequently form between segments. This transition can increase further resistance to stretching, although in

this study, “unfolding” is considered to occur before this transition happens to prevent including bond-stretching energy associated with straining the backbone. Overall, while keratin begins with a larger initial length, CsgA and CsgB unfold to nearly 10 times larger strains than keratin. The keratin helices contain 90 and 95 residues, respectively, while CsgA and CsgB contain 131 and 130 residues. The initial structures of CsgA and CsgB, however, contain fewer backbone hydrogen bonds normalized by number of helical residues (0.34 and 0.47, respectively), compared with the 1coi alpha helix (0.55) and keratin (0.7). While nearly each amino acid within an alpha helix (aside from the termini) is aligned with an adjacent residue to form a hydrogen bond, when excluding turn regions and the unstructured N-terminus from the beta-helices studied, only about 80 amino acids are expected to form a beta-structure

Given these differences, we normalize the work to unfold each protein by these measures, which can be found in Table 2 and Fig 3. Keratin has a higher initial length, number of hydrogen bonds, and number of residues than the beta-helices tested. Because of this, normalizing work based on factors such as backbone hydrogen bonds, residues, and initial length result in CsgB requiring most normalized work to unfold, followed by CsgA, keratin, and finally the single alpha helix. Normalizing based on factors relating to the

	Total Work (kcal/mol)	Normalized Work					
		Initial Length (kcal/mol/Å)	Extended Length (kcal/mol/Å)	Strain (kcal/mol)	#BB HBs (kcal/mol)	# Residues (kcal/mol)	δ Length (kcal/mol/Å)
CsgA	1152.0	47.5	2.3	59.0	30.3	8.8	2.4
CsgB	1411.7	58.6	2.9	72.4	27.7	10.9	3.0
α -helix (1coi)	102.8	2.6	0.9	57.0	6.4	3.5	1.4
Keratin	1273.4	9.4	3.5	765.1	9.7	6.9	5.6

Table 2. Normalized work to unfold for each protein tested.

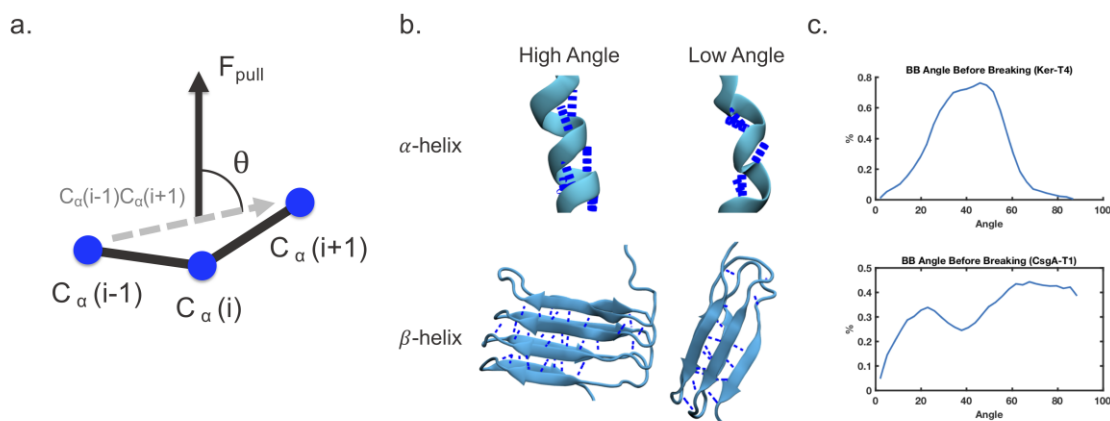


Figure 4. Difference in angle between backbone alpha carbon vectors and applied pulling force. Schematic of angle measured (a), renderings of examples of high and low angles for both alpha and beta helices (b), distribution of backbone alpha carbon vectors in the moments before hydrogen bond breakage (c).

extended length produce the order: keratin > CsgB > CsgA > alpha helix. Although initial and final length (and strain) are geometry based, the work to unfold does not scale directly with number of residues or hydrogen bonds, indicating differences in energy dissipation are not purely due to size (mass), but to composition or form as well. So far, there is no direct explanation as to why these may be higher for one structural motif over another.

Factors that may contribute to stabilization of the helices tested here include hydrophobic effects, “zippered” or interlocking side chains, electrostatic effects, and hydrogen bond cooperativity. The impact of sequence chemistry on work to unfold can be observed when comparing the beta-helices CsgA and CsgB, which contain varying sequences yet similar size and geometry. Both CsgA and CsgB contain two sets of inward-facing conserved hydrophobic residues on each beta-sheet face (for four sets total). CsgA has a total of 19 inward facing hydrophobic residues within the helix core, and CsgB has 21 total inward facing hydrophobic residues. Within the same beta-sheet face, CsgA only has four outward-facing hydrophobic residues compared to twelve outward-facing residues in CsgB, which are mostly concentrated on the same sheet. As previous papers have noted the stabilizing effect of hydrophobic amino acids⁴⁰⁻⁴², additional hydrophobic residues may contribute to the larger amount of the work required to unfold CsgB compared to CsgA. However, the work to unfold of CsgA and CsgB is not proportional to the number of hydrophobic residues (either inward, outward, or total), so it is not straightforward to attribute this difference solely to hydrophobicity. CsgA and CsgB have similar numbers of charged residues within the helix core: 14 total for CsgA (4 positive, 10 negative) and 15 total for CsgB (10 positive, 5 negative). Despite similar total numbers of charged residues, the distribution of charged residues differs between CsgA and CsgB, with CsgB having fewer instances of neighboring or nearby like charges and more instances of neighboring or nearby opposite charges than in CsgA. Both hydrophobic and electrostatic contributions likely contribute to this difference between CsgA and CsgB.

Within alpha-helical assemblies, leucine zippers have shown to stabilize coiled coil structures^{43, 44}. Indeed, in the keratin dimer

tested, 22 total leucines in both segments were near or interlocking with leucines in the adjacent segment. Similarly, the keratin dimer contains 7 compatible charge pairs (although two residues are each involved in two pairs). There is one case of same charges in proximity to one another. Within the keratin dimer, although leucine pairs and charged pairs are found throughout the length of both helices, there are two particular regions with multiple (>3) adjacent or nearby sets of pairs. Indeed, in these clustered segments we see unfolding occur last, demonstrating the stabilizing effects of hydrophobic and compatibly charged interactions between the keratin helices. Within the last 20% of the protein lifetime, the remaining hydrogen bonds are either directly within these two clusters or nearby (within 5 residues). Lastly, although disulfide bonds can be stabilizing in coiled coils⁴⁵, no cysteine residues are located proximally to one another within this keratin structure that could lead this to be a stabilizing factor.

Hydrogen bond cooperativity has also been identified as a stabilizing effect in proteins, arising from “non-additivity” in hydrogen bonds, where the strength per hydrogen bonds is higher in a group than individually⁴⁶. While hydrogen bond cooperativity has been noted in alpha-helices, its presence in beta-sheet structures has been debated⁴⁷⁻⁴⁹. Studies that suggest cooperativity among hydrogen bonds in beta-sheet structures have found cooperativity in directions perpendicular to the beta-strand and increasing with size⁴⁹⁻⁵¹. Hydrogen bond cooperativity depends on protein geometry, is generally difficult to quantify, and has been reported more often for alpha-helical structures than beta-helices^{47, 52}. In spite of this, the beta-helical proteins tested here achieved larger normalized work to unfold than alpha-helices. The cooperativity among hydrogen bonds in both helical structures may incur additional energy barriers of varying magnitude to unfold the proteins, leading to disparate work to unfold per hydrogen bond based on structural motif. Additionally, a rate dependence has been found in hydrogen bond breakage, where at low speeds/forces hydrogen bonds rupture simultaneously, while at high speeds hydrogen bonds break sequentially⁵³.

Mechanism Differences – Backbone Angle

To further investigate differences in energy dissipation, we focus on geometry during unfolding. As observed in snapshots of each helix during unfolding (see Fig S1), the shorter, wider beta helices rotate to larger angles during unfolding. To study the impact of this on unfolding, we measure the angle between each backbone vector and the pulling direction for each residue in the helix core, as seen in the schematic of Fig 4a. Examples of protein backbone and hydrogen bond alignment at low and high angles for both alpha and beta helices are shown in Fig 4b. Instances of low angles between the backbone and pulling vector generally occur during instances of high angles between the hydrogen bonds and pulling vector, and representative plots of average hydrogen bond angle versus extension can be found in Fig S7. The distribution of angles between each backbone vector and the pulling direction in the last 0.2 ns before that strand is peeled from the helix core are plotted for a representative trial (the trial requiring largest work to unfold) for CsgA and keratin in Fig 4c. For keratin, one broad peak is visible, with the majority of backbone angles being between 30-50 degrees. Due to alpha-helix geometry, the backbone is rarely orthogonal to the pulling direction, limiting exposure of higher angles. At the same time, rotation of the backbone involved in breaking a hydrogen bond is much less than in shorter, wider helices, such that the backbone is also rarely colinear with the pulling direction when separated from the helix core. Alternatively, CsgA often has two peaks in backbone angle distribution as backbone hydrogen bonds are broken. The higher angles represent when the core of the helix is situated such that beta-strands are orthogonal to the pulling direction and strands are peeled from the core. This appears early in unfolding, when fewer strands have separated and the helix core cannot rotate to as large angles. Once multiple strands have been peeled from the core, the beta-strands align to the pulling direction at lower angles, representing strands being sheared away. The beta-helix exhibits rigid body rotations under applied force to align strands with the pulling direction, exhibiting lower backbone angles between the force and the backbone as the deformation proceeds. Separating beta-strands in shear has already been noted to require larger fracture forces than by separation due to peeling⁵⁴. Although keratin has little difference between individual trials in the distribution of backbone angles, individual beta-helical trials vary in regard to proportion of peak heights, and trials with a flatter distribution require lower work to unfold. Beta-helical trials requiring the most work to unfold possess larger proportions of low backbone angles and high hydrogen bonds (shearing) compared to low backbone angles (shearing).

Conclusions

We present evidence suggesting how helix geometry and backbone influence work to unfold proteins under tensile deformations. We find a similar amount of total work is needed to unfold alpha and beta-helices within the same size range (100-200 amino acids). However, beta-helices require more work per hydrogen bond or number of residues to fully unfold the protein. To explain this, we examine the mechanisms of backbone separation during unfolding and find that the geometry of beta-helices is conducive to increasing energy dissipation during extension. The larger ratio of width to height results in increasingly large rotations during subsequent strand peeling, leading to hydrogen bonds being broken in shear or out of plane peeling rather than in-plane peeling. This mechanism enhances the resistance to unfolding. The most conclusive finding is the observation that beta-helices, owing to their larger radius, pack more hydrogen bonds to a given end-to-end length distance, which

gives them more extensibility and more work dissipated per initial length.

These findings underline the importance of geometry in design of unfolding-resistant structures. The results of this study pertain to single monomers under tensile load, and this behavior could vary when assembled in a fibril due to different loading conditions at either terminus. This work corroborates other findings concerning dependence of work to unfold on protein size and pulling rate, while revealing new differences in energy dissipation during mechanical unfolding. The geometric influence of helix width and height implies that proteins under applied tensile load may be designed for optimal unfolding resistance based on geometry. The number of turns (height) and helix radius could be tuned to maximize unfolding resistance and could be further constrained by the maximum deformation allowed before separation should occur. This further connects protein structure to mechanical properties and therefore function. These findings are of importance for considerations in engineered proteins, either by design of synthetic proteins or to guide selection criteria in using existing proteins within hybrid/conjugated materials. Gels formed from networks of either alpha and beta-helical motifs or their combinations could exhibit diverse mechanical responses and exhibit very high toughness due to the high energy dissipation capacity of these systems. Further questions of interest in future research could focus on optimizing length/width parameters in beta-helical proteins, using 3-faced solenoid structures rather than two, and incorporating protein-protein interfaces under applied load to represent monomers within an assembled structure.

Conflicts of interest

There are no conflicts to declare.

Acknowledgements

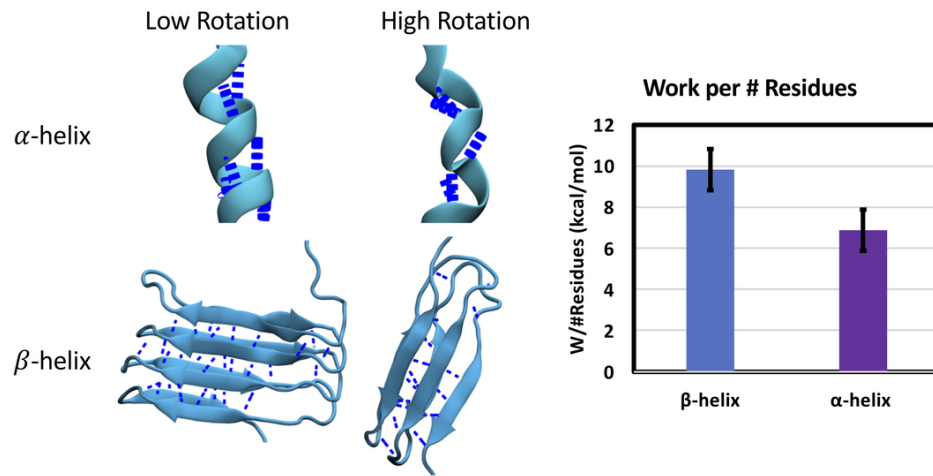
The authors acknowledge a supercomputing grant from the Northwestern University High Performance Computing Center and the Department of Defense Supercomputing Resource Center. E.P.D. gratefully acknowledges support from the Ryan Fellowship and the Northwestern University International Institute for Nanotechnology. This research was sponsored by an award from the Office of Naval Research Young Investigator Program (grant #N00014-15-1-2701). E.P.D was additionally sponsored with Government support under and awarded by DoD, Air Force Office of Scientific Research, National Defense Science and Engineering Graduate (NDSEG) Fellowship, 32 CFR 168a.

References

1. Ackbarow, T.; Sen, D.; Thaulow, C.; Buehler, M. J., Alpha-helical protein networks are self-protective and flaw-tolerant. *PLoS One* **2009**, *4* (6), e6015.
2. Shin, J. H.; Gardel, M.; Mahadevan, L.; Matsudaira, P.; Weitz, D., Relating microstructure to rheology of a bundled and cross-linked

- F-actin network in vitro. *Proceedings of the National Academy of Sciences* **2004**, *101* (26), 9636-9641.
3. Rohs, R.; Etchebest, C.; Lavery, R., Unraveling proteins: a molecular mechanics study. *Biophysical journal* **1999**, *76* (5), 2760-2768.
 4. Brockwell, D. J.; Paci, E.; Zinober, R. C.; Beddard, G. S.; Olmsted, P. D.; Smith, D. A.; Perham, R. N.; Radford, S. E., Pulling geometry defines the mechanical resistance of a β -sheet protein. *Nature Structural and Molecular Biology* **2003**, *10* (9), 731.
 5. Zhmurov, A.; Kononova, O.; Litvinov, R. I.; Dima, R. I.; Barsegov, V.; Weisel, J. W., Mechanical transition from α -helical coiled coils to β -sheets in fibrin (ogen). *Journal of the American Chemical Society* **2012**, *134* (50), 20396-20402.
 6. Feughelman, M., *Mechanical properties and structure of alpha-keratin fibres: wool, human hair and related fibres*. UNSW press: 1997.
 7. Root, D. D.; Yadavalli, V. K.; Forbes, J. G.; Wang, K., Coiled-coil nanomechanics and uncoiling and unfolding of the superhelix and α -helices of myosin. *Biophysical journal* **2006**, *90* (8), 2852-2866.
 8. Rief, M.; Pascual, J.; Saraste, M.; Gaub, H. E., Single molecule force spectroscopy of spectrin repeats: low unfolding forces in helix bundles. *Journal of molecular biology* **1999**, *286* (2), 553-561.
 9. Wang, N.; Stamenovic, D., Mechanics of vimentin intermediate filaments. *Journal of Muscle Research & Cell Motility* **2002**, *23* (5-6), 535-540.
 10. Keten, S.; Buehler, M. J., Large deformation and fracture mechanics of a beta-helical protein nanotube: Atomistic and continuum modeling. *Computer Methods in Applied Mechanics and Engineering* **2008**, *197* (41-42), 3203-3214.
 11. Liou, Y.-C.; Tocilj, A.; Davies, P. L.; Jia, Z., Mimicry of ice structure by surface hydroxyls and water of a β -helix antifreeze protein. *Nature* **2000**, *406* (6793), 322.
 12. Simkovsky, R.; King, J., An elongated spine of buried core residues necessary for in vivo folding of the parallel β -helix of P22 tailspike adhesin. *Proceedings of the National Academy of Sciences* **2006**, *103* (10), 3575-3580.
 13. Steinbacher, S.; Baxa, U.; Miller, S.; Weintraub, A.; Seckler, R.; Huber, R., Crystal structure of phage P22 tailspike protein complexed with Salmonella sp. O-antigen receptors. *Proceedings of the National Academy of Sciences* **1996**, *93* (20), 10584-10588.
 14. Chapman, M. R.; Robinson, L. S.; Pinkner, J. S.; Roth, R.; Heuser, J.; Hammar, M.; Normark, S.; Hultgren, S. J., Role of Escherichia coli curli operons in directing amyloid fiber formation. *Science* **2002**, *295* (5556), 851-855.
 15. Keten, S.; Alvarado, J. F. R.; Müftü, S.; Buehler, M. J., Nanomechanical characterization of the triple β -helix domain in the cell puncture needle of bacteriophage T4 virus. *Cellular and Molecular Bioengineering* **2009**, *2* (1), 66-74.
 16. Zhong, C.; Gurry, T.; Cheng, A. A.; Downey, J.; Deng, Z.; Stultz, C. M.; Lu, T. K., Strong underwater adhesives made by self-assembling multi-protein nanofibres. *Nature nanotechnology* **2014**, *9* (10), 858-866.
 17. Nguyen, P. Q.; Botyanszki, Z.; Tay, P. K. R.; Joshi, N. S., Programmable biofilm-based materials from engineered curli nanofibres. *Nature communications* **2014**, *5*, 4945.
 18. Zhang, C.; Li, Y.; Wang, H.; He, S.; Xu, Y.; Zhong, C.; Li, T., Adhesive Bacterial Amyloid Nanofibers-Mediated Growth of Metal-Organic Frameworks on Diverse Polymeric Substrates. *Chemical Science* **2018**, *9*, 5672-5678.
 19. Axpe, E.; Duraj-Thatte, A.; Chang, Y.; Kaimaki, D.-M.; Sanchez-Sanchez, A.; Caliskan, H. B.; Dorval Courchesne, N. m.-M.; Joshi, N. S., Fabrication of amyloid curli fibers-alginate nanocomposite hydrogels with enhanced stiffness. *ACS Biomaterials Science & Engineering* **2018**, *4* (6), 2100-2105.
 20. Baclayon, M.; Ulsen, P. v.; Mouhib, H.; Shabestari, M. H.; Verzijden, T.; Abeln, S.; Roos, W. H.; Wuite, G. J., Mechanical unfolding of an autotransporter passenger protein reveals the secretion starting point and processive transport intermediates. *ACS nano* **2016**, *10* (6), 5710-5719.
 21. Kim, M.; Abdi, K.; Lee, G.; Rabbi, M.; Lee, W.; Yang, M.; Schofield, C. J.; Bennett, V.; Marszalek, P. E., Fast and forceful refolding of stretched α -helical solenoid proteins. *Biophysical journal* **2010**, *98* (12), 3086-3092.
 22. Alsteens, D.; Martinez, N.; Jamin, M.; Jacob-Dubuisson, F., Sequential unfolding of beta helical protein by single-molecule atomic force microscopy. *PLoS One* **2013**, *8* (8), e73572.
 23. Barbirz, S.; Becker, M.; Freiberg, A.; Seckler, R., Phage Tailspike Proteins with β -Solenoid Fold as Thermostable Carbohydrate Binding Materials. *Macromolecular bioscience* **2009**, *9* (2), 169-173.
 24. Peng, Z.; Parker, A. S.; Peralta, M. D.; Ravikumar, K. M.; Cox, D. L.; Toney, M. D., High Tensile Strength of Engineered β -Solenoid Fibrils via Sonication and Pulling. *Biophysical journal* **2017**, *113* (9), 1945-1955.
 25. Qin, Z.; Kreplak, L.; Buehler, M. J., Nanomechanical properties of vimentin intermediate filament dimers. *Nanotechnology* **2009**, *20* (42), 425101.
 26. Buehler, M. J.; Keten, S., Elasticity, strength and resilience: A comparative study on mechanical signatures of α -helix, β -sheet and tropocollagen domains. *Nano Research* **2008**, *1* (1), 63.
 27. Solar, M.; Buehler, M. J., Comparative analysis of nanomechanics of protein filaments under lateral loading. *Nanoscale* **2012**, *4* (4), 1177-1183.
 28. Solar, M.; Buehler, M. J., Tensile deformation and failure of amyloid and amyloid-like protein fibrils. *Nanotechnology* **2014**, *25* (10), 105703.
 29. Qin, Z.; Kreplak, L.; Buehler, M. J., Hierarchical structure controls nanomechanical properties of vimentin intermediate filaments. *PLoS one* **2009**, *4* (10), e7294.
 30. Heinz, L. P.; Ravikumar, K. M.; Cox, D. L., In silico measurements of twist and bend moduli for β -solenoid protein self-assembly units. *Nano letters* **2015**, *15* (5), 3035-3040.
 31. Cieplak, M.; Hoang, T. X.; Robbins, M. O., Thermal folding and mechanical unfolding pathways of protein secondary structures. *Proteins: Structure, Function, and Bioinformatics* **2002**, *49* (1), 104-113.
 32. Ackbarow, T.; Chen, X.; Keten, S.; Buehler, M. J., Hierarchies, multiple energy barriers, and robustness govern the fracture mechanics of α -helical and β -sheet protein domains. *Proceedings of the National Academy of Sciences* **2007**, *104* (42), 16410-16415.
 33. DeBenedictis, E.; Ma, D.; Keten, S., Structural predictions for curli amyloid fibril subunits CsgA and CsgB. *RSC Advances* **2017**, *7* (76), 48102-48112.
 34. Phillips, J. C.; Braun, R.; Wang, W.; Gumbart, J.; Tajkhorshid, E.; Villa, E.; Chipot, C.; Skeel, R. D.; Kale, L.; Schulten, K., Scalable molecular dynamics with NAMD. *Journal of computational chemistry* **2005**, *26* (16), 1781-1802.
 35. Vanommeslaeghe, K.; Hatcher, E.; Acharya, C.; Kundu, S.; Zhong, S.; Shim, J.; Darian, E.; Guvench, O.; Lopes, P.; Vorobyov, I., CHARMM general force field: A force field for drug-like molecules compatible with the CHARMM all-atom additive biological force fields. *Journal of computational chemistry* **2010**, *31* (4), 671-690.
 36. Best, R. B.; Zhu, X.; Shim, J.; Lopes, P. E.; Mittal, J.; Feig, M.; Mackerell Jr, A. D., Optimization of the additive CHARMM all-atom protein force field targeting improved sampling of the backbone ϕ ,

- ψ and side-chain χ_1 and χ_2 dihedral angles. *Journal of chemical theory and computation* **2012**, *8* (9), 3257-3273.
37. Essmann, U.; Perera, L.; Berkowitz, M. L.; Darden, T.; Lee, H.; Pedersen, L. G., A smooth particle mesh Ewald method. *The Journal of chemical physics* **1995**, *103* (19), 8577-8593.
38. Park, S.; Schulten, K., Calculating potentials of mean force from steered molecular dynamics simulations. *The Journal of chemical physics* **2004**, *120* (13), 5946-5961.
39. Humphrey, W.; Dalke, A.; Schulten, K., VMD: visual molecular dynamics. *Journal of molecular graphics* **1996**, *14* (1), 33-38.
40. VAN DAN BURG, B.; Dijkstra, B. W.; Vriend, G.; VAN DAR VINNE, B.; Venema, G.; Eijssink, V. G. J. E. J. o. b., Protein stabilization by hydrophobic interactions at the surface. **1994**, *220* (3), 981-985.
41. Tanford, C. J. J. o. t. A. C. S., Contribution of hydrophobic interactions to the stability of the globular conformation of proteins. **1962**, *84* (22), 4240-4247.
42. Doig, A. J.; Williams, D. H. J. J. o. m. b., Is the hydrophobic effect stabilizing or destabilizing in proteins?: The contribution of disulphide bonds to protein stability. **1991**, *217* (2), 389-398.
43. O'Shea, E. K.; Rutkowski, R.; Kim, P. S. J. S., Evidence that the leucine zipper is a coiled coil. **1989**, *243* (4890), 538-542.
44. O'Shea, E. K.; Klemm, J. D.; Kim, P. S.; Alber, T. J. S., X-ray structure of the GCN4 leucine zipper, a two-stranded, parallel coiled coil. **1991**, *254* (5031), 539-544.
45. Feng, X.; Coulombe, P. A. J. J. C. B., A role for disulfide bonding in keratin intermediate filament organization and dynamics in skin keratinocytes. **2015**, *209* (1), 59-72.
46. Nochebuena, J.; Cuautli, C.; Ireta, J., Origin of cooperativity in hydrogen bonding. *Physical Chemistry Chemical Physics* **2017**, *19* (23), 15256-15263.
47. Li, J.; Wang, Y.; Chen, J.; Liu, Z.; Bax, A.; Yao, L., Observation of α -helical hydrogen-bond cooperativity in an intact protein. *Journal of the American Chemical Society* **2016**, *138* (6), 1824-1827.
48. Zhao, Y.-L.; Wu, Y.-D. J. J. o. t. A. C. S., A theoretical study of β -sheet models: is the formation of hydrogen-bond networks cooperative? **2002**, *124* (8), 1570-1571.
49. Rossmeis, J.; Nørskov, J. K.; Jacobsen, K. W. J. J. o. t. A. C. S., Elastic effects behind cooperative bonding in β -sheets. **2004**, *126* (40), 13140-13143.
50. Viswanathan, R.; Asensio, A.; Dannenberg, J., Cooperative hydrogen-bonding in models of antiparallel β -sheets. *The Journal of Physical Chemistry A* **2004**, *108* (42), 9205-9212.
51. Schenck, H. L.; Gellman, S. H., Use of a designed triple-stranded antiparallel β -sheet to probe β -sheet cooperativity in aqueous solution. *Journal of the American Chemical Society* **1998**, *120* (19), 4869-4870.
52. Wieczorek, R.; Dannenberg, J., H-bonding cooperativity and energetics of α -helix formation of five 17-amino acid peptides. *Journal of the American Chemical Society* **2003**, *125* (27), 8124-8129.
53. Ackbarow, T.; Keten, S.; Buehler, M. J. J. o. P. C. M., A multi-timescale strength model of alpha-helical protein domains. **2008**, *21* (3), 035111.
54. Keten, S.; Buehler, M. J., Geometric confinement governs the rupture strength of H-bond assemblies at a critical length scale. *Nano Letters* **2008**, *8* (2), 743-748.



96x48mm (300 x 300 DPI)